EUROPEAN ORGANIZATION FOR NUCLEAR RESEARCH

CERN-EP/90-86
18 June 1990

A study of the centrally produced $\pi^+\pi^-\pi^0$ system formed in the reaction $pp \rightarrow p_f (\pi^+\pi^-\pi^0) p_s$ at 300 GeV/c

WA76 Collaboration

T.A. Armstrong [4,*)], M. Benayoun [5)], W. Beusch [4)], I.J. Bloodworth [3)], J.N. Carney [3)], R. Childs [3)], C. Evangelista [2)], B.R. French [4)], B. Ghidini [2)], M. Girone [2)], A. Jacholkowski [4)], J. Kahane [5)], J.B. Kinson [3)], A. Kirk [4)], K. Knudson [4)], V. Lenti [2)], Ph. Leruste [5)], A. Malamant [5)], J.L. Narjoux [5)], F. Navach [2)], A. Palano [2)], E. Quercigh [4)], N. Redaelli [4,**)], L. Rossi [4,***)], M. Sené [5)], R. Sené [5)], M. Stassinaki [1)], M.T. Trainor [4,†)], G. Vassiliadis [1)], O. Villalobos Baillie [3)] and M.F. Votruba [3)]

Abstract

The reaction $pp \rightarrow p_f(\pi^+\pi^-\pi^0)p_s$, where the $\pi^+\pi^-\pi^0$ system is centrally produced, has been studied at 300 GeV/c. The $\pi^+\pi^-\pi^0$ mass spectrum shows evidence for the η, ω and $a_2(1320)$ as well as an enhancement in the $a_1(1260)$ region. A Dalitz plot analysis of the $\pi^+\pi^-\pi^0$ system has been performed. The $a_1(1260)$ parameters coming from the fit of the 1^+ S wave are m = 1208 ± 15 MeV and Γ = 430 ± 50 MeV. No evidence is found for the $h_1(1170)$ or $h_1(1380)$.

Submitted to Zeitschrift für Physik C

---

1) Athens University, Physics Department, Athens, Greece
2) Dip. di Fisica dell'Università and Sez. INFN, Bari, Italy
3) University of Birmingham, Physics Department, Birmingham,U.K.
4) CERN, CH-1211 Geneva 23, Switzerland
5) Collège de France, Paris, France

*) Present address: Pennsylvania State University, University Park, USA
**) Present address: INFN and Dip. di Fisica, Milan, Italy
***) Present address: INFN and Dip. di Fisica, Genoa, Italy
†) Present address: Oxford University, Oxford, U.K.

1. Introduction

The parameters of the isovector member of the $J^{PC} = 1^{++}$ nonet, the $a_1(1260)$, have been a long-standing question. The extraction of the parameters of the a_1 from its production in π^-p hadronic interactions and its decay to $\rho\pi$ have been hampered by the presence of a Deck background [1]. This problem in fact called into question the very existence of the a_1 as a resonance. The existence of the a_1 was settled primarily by two high statistics experiments dealing with diffractive [2] and charge exchange [3] production of the 3π system in π^-p interactions. The behaviour of the 1^+ S $(\rho\pi)$ amplitude requires the presence of both a Deck background and a resonance. The parameters from these two experiments give an average a_1 mass of 1275 ± 28 MeV and a width of 316 ± 45 MeV [4].

New experiments studying the process $\tau \rightarrow a_1(1260)\nu \rightarrow \rho\pi\nu$ [5], which is free from the Deck effect, have given different parameters for the a_1. However these sets of data have been reanalysed and give $m(a_1) = 1235 \pm 40$ MeV, $\Gamma(a_1) = 400 \pm 100$ MeV [6] and $m(a_1) = 1250 \pm 40$ MeV, $\Gamma(a_1) = 600 \pm 100$ MeV [7].

It should be noted that in a backward produced 3π system in the reaction $K^-p \rightarrow \Sigma^-\pi^+\pi^-\pi^+$, which should be free from the Deck effect, a lower mass $J^{PC} = 1^{++}$ state is observed with m = 1041 ± 13 MeV and Γ = 230 ± 50 MeV [8]. Further confusion comes from a study of the $\pi^+\pi^-\pi^0$ system produced in a recent experiment on π^-p charge exchange [9] where, despite using a fit which takes into account the Deck effect the a_1 mass was found to be in the 1.1 GeV region.

This paper studies, for the first time with significant statistics, the centrally produced exclusive final states formed in the reaction

$$pp \rightarrow p_f (\pi^+\pi^-\pi^0) p_s \qquad (1)$$

at 300 GeV/c, where the subscripts f and s indicate the fastest and slowest particles in the laboratory respectively. The data come from experiment WA76 which has been performed using the CERN Omega Spectrometer. Details of the layout of the apparatus, the trigger conditions and the data processing have been given in a previous publication [10]. The γ's have been detected using the Geneva Photon Detector (GPD) [11] and the Omega Plug gamma calorimeter (PLUG) [12].

2. Selection of the reaction $pp \rightarrow p_f (\pi^+\pi^-\pi^0) p_s$

Reaction (1) has been isolated from the sample of events having four outgoing charged tracks plus two γ's with energy greater than 1 GeV deposited in the electromagnetic calorimeter, by first imposing the following cuts on the components of missing momentum: |missing P_x| < 30.0 GeV/c, |missing P_y| < 0.16 GeV/c, |missing P_z| < 0.08 GeV/c, where the x axis is along the beam direction. Showers associated with charged track impacts on the gamma calorimeters have been removed.

The effective mass of the two γ's is shown in fig. 1 where a clear π^0 signal can be seen which was selected by requiring $0.1 < m(\gamma\gamma) < 0.17$ GeV. After selecting the π^0 events the energies of the γ's were recalculated to give the π^0 mass.

The central charged particles are required, if passing through the Cerenkov system, to have a mass consistent with being a pion. The Delta function defined as

$$\Delta = MM^2(p_f p_s) - M^2(\pi^+\pi^-\pi^0)$$

is then calculated for each event and a cut of $|\Delta| \leq 3.0$ GeV^2 is used to select the $\pi^+\pi^-\pi^0$ channel (24972 events).

The centre of mass rapidity distribution (y_{π^0}) for the π^0 is shown in fig. 2a where two peaks can be seen. The effective mass of the fast proton and the π^0 is shown in fig. 3a where a clear Δ^+ signal can be seen. The shaded area in fig. 3a is produced by requiring $y_{\pi^0} < 1.7$. Hence the diffractive π^0 contribution can be removed by a suitable cut in rapidity. Fig. 2b shows the corresponding rapidity for the π^+, no clear double peaked structure can be seen since the majority of the diffractively produced π^+'s are removed by the trigger. However again requiring $y_{\pi^+} < 1.7$ removes the remaining Δ^{++} signal as is shown in fig. 3b. Figs. 2c and 3c show the rapidity of the π^- and the effective mass of the π^- and fast proton respectively. There is no signal of Δ^0 production and therefore no cut is made on the rapidity of the π^-. Fig. 4 shows the Feynman x distribution after the cuts described above. The central system is well separated from the fast and slow particles. The rapid decrease in the number of π^0's for $y_{\pi^0} < 0$ in fig. 2a is due to the acceptance of the electromagnetic calorimeter.

Fig. 5a shows the $\pi^+\pi^-$ mass spectrum for those events having $y_{\pi^0} > 1.7$. A clear $\rho^0(770)$ signal can be seen corresponding to the $\Delta^+\rho^0$ channel. Fig. 5b and c show the $\pi^\pm\pi^0$ and $\pi^+\pi^-$ mass spectra

respectively remaining after the diffractive contributions have been removed by the above rapidity cuts. There is a clear excess of $\rho^{\pm}$ events over ρ^0 events. The simplest way to explain this excess is that most of the $\rho^{\pm}$'s are coming from the decay of an I = 1 system, since an isovector state can not decay to $\rho^0\pi^0$.

3. The $\pi^+\pi^-\pi^0$ mass spectrum

Fig. 6a shows the resulting centrally produced $\pi^+\pi^-\pi^0$ mass spectrum; the η and ω can clearly be seen. There is also some evidence for the $a_2(1320)$. The spectrum has been fitted using a Gaussian to describe the η, a convoluted Breit-Wigner and Gaussian to describe the ω and a spin 2 relativistic Breit-Wigner to describe the $a_2(1320)$ together with a background of the form $(m-m_{th})^{\alpha}\exp(-\beta m-\gamma m^2)$, where m is the $\pi^+\pi^-\pi^0$ mass, m_{th} is the $\pi^+\pi^-\pi^0$ threshold mass and α, β, γ are fit parameters. The fit is shown in fig. 6a where an excess of events in the 1.1 GeV region can be seen. This excess could be due to the presence of the $a_1(1260)$. Therefore the $\pi^+\pi^-\pi^0$ mass spectrum has been refitted by introducing a Breit-Wigner to describe the structure in the 1.1 GeV region using an expression of the form

$$\frac{dN}{dm} = \frac{m_{a_1}\Gamma_{a_1}(m)}{(m^2 - m^2_{a_1})^2 + \Gamma^2_{a_1}(m)m^2_{a_1}}$$

where $\Gamma_{a_1}(m)$ is a mass dependent width of the form

$$\Gamma_{a_1}(m) = \Gamma_{a_1}(m_{a_1}) \frac{\rho^{1^+S}(m)}{\rho^{1^+S}(m_{a_1})} .$$

where $\rho^{1^+S}(m)$ is the phase space for S-wave $\rho^{\pm}(770)\pi^{\mp}$, including the effects of the mass dependent $\rho^{\pm}(770)$ width and of interference between the two $\rho^{\pm}(770)$ bands in the Dalitz plot [6].

Fig. 6b shows the fit which has a χ^2/NDF of 99/63 compared to 193/66 when the Breit-Wigner describing the structure in the 1.1 GeV region is excluded. The parameters of the fit including the

Breit-Wigner described above are given in table 1. The mass found for the structure in the 1.1 GeV mass region (1108 ± 16 MeV) is somewhat lower than the PDG average for the $a_1(1260)$ [13]. However since there may be many processes contributing to the $\pi^+\pi^-\pi^0$ mass spectrum the parameters of the $a_1(1260)$ are best determined from a fit to the 1^+ S wave which is described in the following section.

The geometrical acceptance has been calculated and varies smoothly as a function of the $\pi^+\pi^-\pi^0$ mass. The corrected mass spectrum has also been fitted as described above but no significant changes in the fit parameters are found.

4. Dalitz plot analysis of the $\pi^+\pi^-\pi^0$ system

A Dalitz plot analysis of the $\pi^+\pi^-\pi^0$ mass spectrum has been performed using Zemach tensors and a standard isobar model [14]. The analysis has assumed $\rho(770)$, $f_2(1270)$ and $f_0(1400)$ intermediate states and both I = 0 and 1 have been considered for those states which decay to $\rho^{\pm}(770)\pi^{\mp}$. Waves with spin up to two have been considered.

The $\pi^+\pi^-\pi^0$ mass spectrum has been fitted in 40 MeV bins from 0.86 to 1.94 GeV. A fit using 1^{++} S ($\rho^{\pm}\pi^{\mp}$), 2^{++} D ($\rho^{\pm}\pi^{\mp}$), 1^{--} P ($\rho\pi$) and 2^{-+} S ($f_2(1270)\pi^0$) waves and phase space only are found to describe the data well. The results of the fit are shown in fig. 7.

The 2^{++} D wave shows a peak in the $a_2(1320)$ region and has been fitted using a Breit-Wigner and a flat background giving $m(a_2) = 1310 \pm 5$ MeV, $\Gamma(a_2) = 120 \pm 10$ MeV, values which are consistent with the parameters found from the fit to the mass spectrum.

The 1^{++} S wave shows a broad enhancement. It has been fitted using the Breit-Wigner described above and gives : m = 1208 ± 15 MeV, Γ = 430 ± 50 MeV, parameters which are consistent with the PDG values for the $a_1(1260)$ [13].

It is interesting to note that no 1^{+-} wave is required in the fit, in particular there is no evidence for the $h_1(1170)$ or $h_1(1380)$.

The geometrical acceptance of the apparatus has also been evaluated over the Dalitz plot of the $\pi^+\pi^-\pi^0$ system in 0.1 GeV intervals between 0.8 and 2.0 GeV. The fits have been repeated on the acceptance corrected data but the results obtained above are not changed significantly.

5. Discussion of the production mechanism

The $\pi^+\pi^-\pi^0$ channel has been studied as a function of the four-momentum transferred at the fast (t_1) and slow (t_2) vertices (see fig 8). Fig. 9a,b shows the $\pi^+\pi^-\pi^0$ mass spectra at low ($t < 0.3$ GeV^2) and high ($t > 0.3$ GeV^2) four-momentum transfer.

The number of events associated with each resonance, corrected for geometrical acceptance, has been calculated in the two t regions. The fraction of each resonance compared to the amount of $\omega(783)$ in each region has been calculated and is shown in table 2. It is interesting to note that the η is suppressed relative to the $\omega(783)$ at low t whereas the opposite is true for the $a_1(1260)$.

In reaction (1), since the incident and outgoing particles at the top and bottom vertices are both protons the isospin of the exchanged particles can be 1 or 0. However the third component of the isospin must be 0. Since two $I = 1$, $I_3 = 0$ exchanged particles cannot produce an $I = 1$ state, the $I = 1$ central states observed in this reaction must be due to an $I = 1$ particle being exchanged from one vertex and an $I = 0$ particle being exchanged form the other. On the other hand the $I = 0$ states observed could be produced by either $I = 1$ or $I = 0$ exchange from both vertices.

These points can be investigated by studying the reaction

$$pp \rightarrow \Delta^+_f(\pi^+\pi^-\pi^0)p_s \qquad (2)$$

where the Δ^+_f is observed to decay to a fast proton and π^0 which are both detected. In this case the particle exchanged from the fast vertex must have $I = 1$. Reaction (2) has been isolated from the sample of events having four outgoing charged tracks plus four γ's with energy greater than 1 GeV deposited in the electromagnetic calorimeter, by first imposing the following cuts on the components of missing momentum: |missing P_x| < 30.0 GeV/c, |missing P_y| < 0.16 GeV/c, |missing P_z| < 0.08 GeV/c, where the x axis is along the beam direction. Showers associated with charged track impacts on the gamma calorimeters have been removed.

Fig. 10a shows the scatter diagram of $m(\gamma_1\gamma_2)$ vs $m(\gamma_3\gamma_4)$ where a clear peak is visible corresponding to the $\pi^0\pi^0$ events which is selected by requiring $0.1 < m(\gamma\gamma) < 0.17$ GeV. After selecting the $\pi^0\pi^0$ events the energies of the γ's were recalculated to give the π^0 mass.

The central charged particles are required, if passing through the Cerenkov system, to have a mass consistent with being a pion. The Delta function defined as

$$\Delta = MM^2(p_f p_s) - M^2(\pi^+\pi^-\pi^0\pi^0)$$

is then calculated for each event and a cut of $|\Delta| \leq 3.0$ GeV^2 is used to select the $\pi^+\pi^-\pi^0\pi^0$ channel. Diffractive Δ^{++} are removed by requiring $y_{\pi^+} < 1.7$ as in reaction (1). The effective mass of the fast proton and one of the π^0's is shown in fig. 10b where a clear Δ^+ signal can be seen. The shaded area in fig. 10b is produced by requiring $y_{\pi^0} > 1.7$. Hence reaction (2) can be selected by requiring one and only one of the π^0's to have $y_{\pi^0} > 1.7$.

The centrally produced mass spectrum for reaction (2) is shown in fig. 11 where it has been fitted using the parameters given in table 1. It is interesting to note that the I = 0 states are suppressed relative to the I = 1 states compared with what is observed in reaction (1). This indicates that the strong ω and η signals seen in reaction (1) are produced by I = 0 exchange from both vertices.

Since in reaction (2) a fast Δ^+ is observed the amount of slow Δ^+ contamination to reaction (1) has been investigated where a slow π^0 from the decay of the Δ^+ falls within the missing momentum cuts. A Monte Carlo simulation has been performed normalising the number of slow Δ^+'s to the number of fast Δ^+'s observed. The fraction of events belonging to reaction (1) that could be associated with a slow Δ^+ is found to be 0.6 %. Hence the I = 1 signals observed can not be accounted for by such a reaction.

Therefore it appears that there is evidence for I = 1 exchange from one of the vertices in the central reactions studied but little evidence for I = 1 exchange from both vertices.

6. Conclusions

In conclusion an analysis of the centrally produced $\pi^+\pi^-\pi^0$ system shows clear η, ω and $a_2(1320)$ production. There is also evidence for isovector production which could be due to the $a_1(1260)$. A Dalitz plot analysis shows a clear $a_2(1320)$ signal in the 2^+ D wave and there is a large 1^+ S wave signal. This 1^+ S wave has been fitted with a single Breit-Wigner only and gives m = 1208 ± 15 MeV and Γ = 430 ± 50 MeV which are consistent with the PDG average for the $a_1(1260)$ [13]. No evidence is found for the $h_1(1170)$ or $h_1(1380)$.

Acknowledgments

We would like to thank Dr. M.G.Bowler for his comments on the analysis presented in this paper.

References

[1] R.T.Deck, Phys. Rev. Lett. **13** (1964) 169.

[2] C.Daum et al., Phys. Lett. **89B** (1980) 281.

C.Daum et al., Nucl. Phys. **B182** (1981) 209.

[3] J.Dankowych et al., Phys. Rev. Lett. **46** (1981) 580.

[4] Particle data group, Phys. Lett. **170B** (1986) 1.

[5] H.Albrecht et al., Z. Phys. **C33** (1986) 7.

W.B.Ruckstuhl et al., Phys. Rev. Lett. **56** (1986) 2132.

W.B.Schmidke et al., Phys. Rev. Lett. **57** (1986) 527.

[6] M.G.Bowler, Phys. Lett. **182B** (1986) 400.

[7] N.A.Tornqvist, Z. Phys. **C36** (1987) 695.

[8] Ph.Gavillet et al., Phys. Lett. **69B** (1977) 119.

[9] A.Ando et al., Proceedings of the Workshop on Glueballs, Hybrids and Exotics, BNL, August 1988.

K.Takamatsu et al., KEK Preprint 89-154 1989.

[10] T.Armstrong et al., Nucl. Instr. and Meth. **A274** (1989) 165.

[11] M.Bonesini et al., Nucl. Instr. and Meth. **A261** (1987) 471.

[12] H.Burmeister et al., Nucl. Instr. and Meth. **A225** (1984) 530.

[13] Particle data group, Phys. Lett. **204B** (1988) 1.

[14] M.Abramovich et al., Nucl. Phys. **B23** (1970) 466.

7. Tables

Table 1: Parameters of resonances in the fit to the $\pi^+\pi^-\pi^0$ mass spectrum

M(η)	547	±	1	MeV
$\sigma(\eta)$	9	±	2	MeV
M(ω)	781	±	1	MeV
$\Gamma(\omega)$	8.5	(fixed)		
$\sigma(\omega)$	15	±	2	MeV
M(a_1)	1108	±	16	MeV
$\Gamma(a_1)$	362	±	55	MeV
M(a_2)	1305	±	5	MeV
$\Gamma(a_2)$	110	±	10	MeV

Table 2: The amount of each resonace normalised to the amount of $\omega(783)$ at low and high t

	Low t	High t
$\eta/\omega(783)$	0.07 ± 0.01	0.15 ± 0.01
$a_1(1260)/\omega(783)$	0.9 ± 0.1	0.47 ± 0.07
$a_2(1320)/\omega(783)$	0.26 ± 0.02	0.25 ± 0.02

8. Figures

Fig. 1 The $\gamma\gamma$ effective mass spectrum.

Fig. 2 The centre of mass rapidity for a) the π^0, b) the π^+ and c) the π^-.

Fig. 3 The a) $p_f\pi^0$, b) $p_f\pi^+$ and c) $p_f\pi^-$ effective mass spectra.

Fig. 4 The Feynman x distribution for the slow, central and fast systems.

Fig. 5 The a) $\pi^+\pi^-$ mass spectrum associated with a Δ^+ and b) $\pi^\pm\pi^0$ and c) $\pi^+\pi^-$ mass spectra after cuts.

Fig. 6 a),b) The $\pi^+\pi^-\pi^0$ mass spectrum with fit described in the text.

Fig. 7 Result of the Dalitz plot analysis. The fit is described in the text.

Fig. 8 Double exchange diagram used to define t_1 and t_2.

Fig. 9 The $\pi^+\pi^-\pi^0$ mass spectrum with fit described in the text. For a) $t < 0.35$ GeV^2 and b) $t > 0.35$ GeV^2.

Fig. 10 a) Scatter plot of $m(\gamma_1\gamma_2)$ vs $m(\gamma_3\gamma_4)$ and

b) the $p_f\pi^0$ effective mass spectra from the reaction $pp \to \pi_f(\pi^+\pi^-\pi^0\pi^0)p_s$. The shaded area corresponds to one of the π^0's having $y_{\pi^0} > 1.7$.

Fig. 11 The $\pi^+\pi^-\pi^0$ mass spectrum from the reaction $pp \to \Delta^+_f(\pi^+\pi^-\pi^0)p_s$ with fit described in the text.

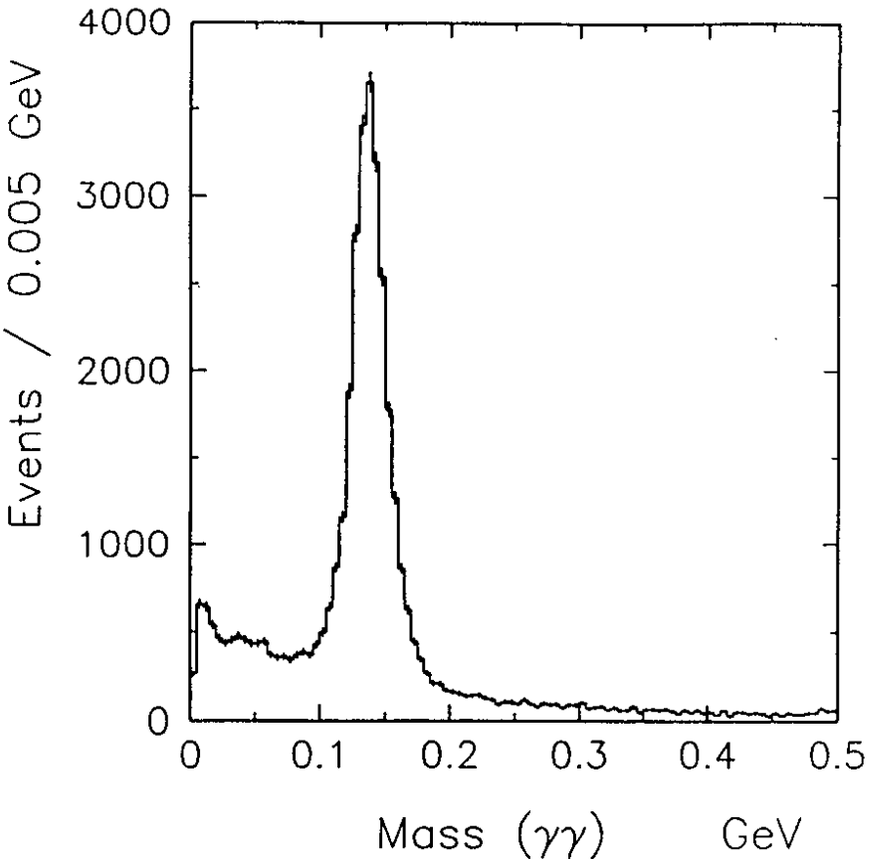
4000
3000
2000
1000
0
Events / 0.005 GeV
0
0.1
0.2
0.3
0.4
0.5
Mass ($\gamma\gamma$) GeV

Fig. 1

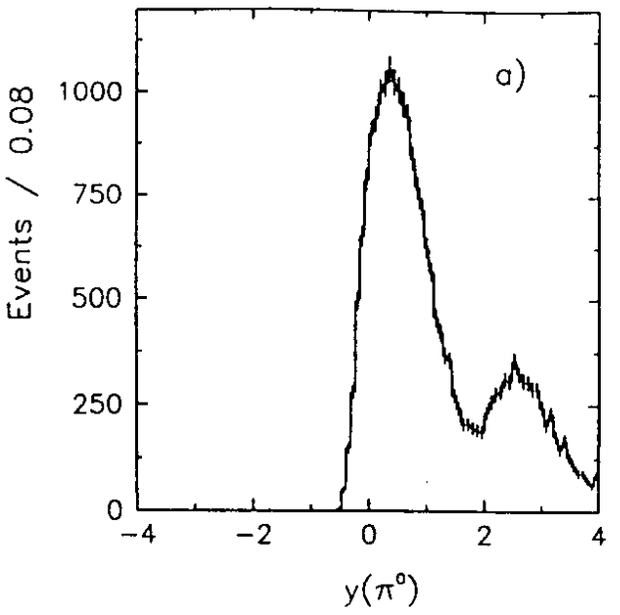
a)
Events / 0.08
1000
750
500
250
0
−4
−2
0
2
4
y(π°)

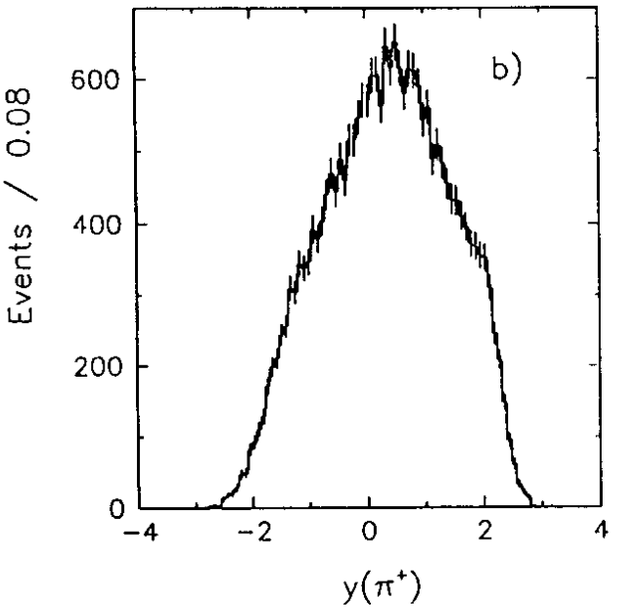
b)
Events / 0.08
600
400
200
0
−4
−2
0
2
4
y(π⁺)

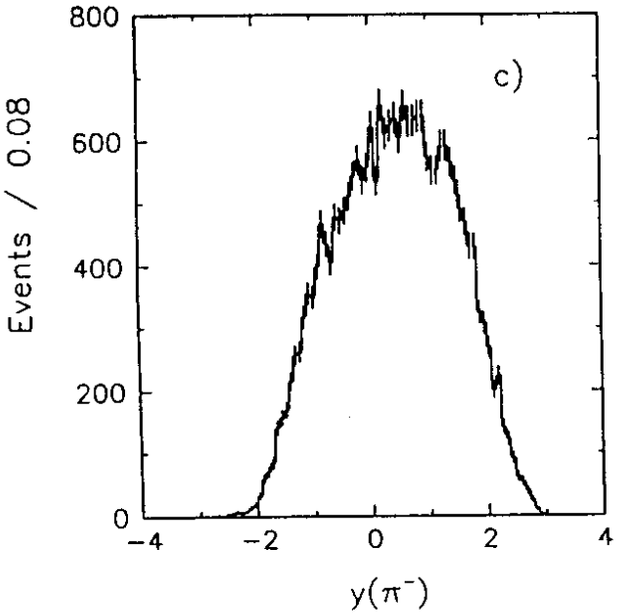
c)
Events / 0.08
800
600
400
200
0
−4
−2
0
2
4
y(π⁻)

Fig. 2

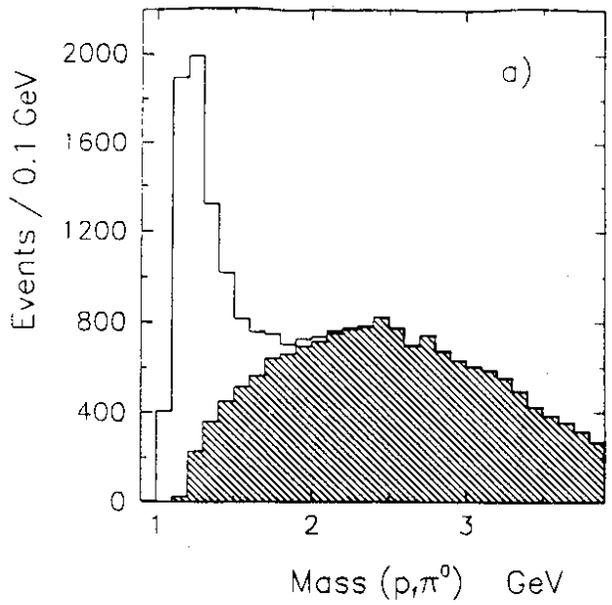
a)
Events / 0.1 GeV
2000
1600
1200
800
400
0
1
2
3
Mass (p,π⁰) GeV

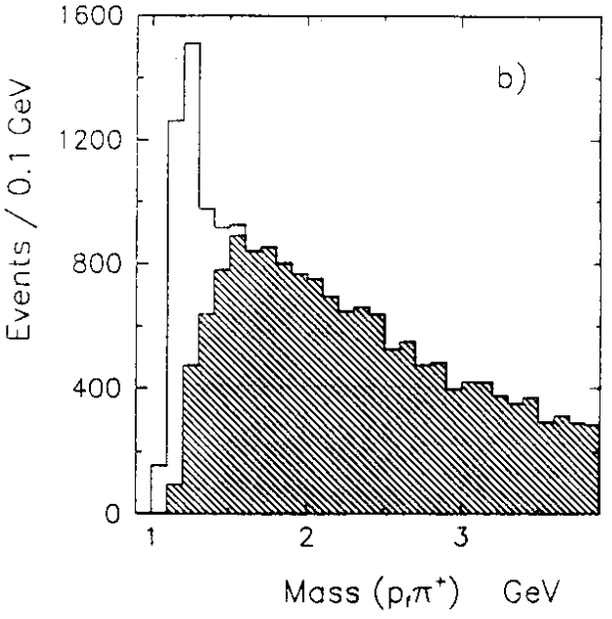
b)
Events / 0.1 GeV
1600
1200
800
400
0
1
2
3
Mass (p,π⁺) GeV

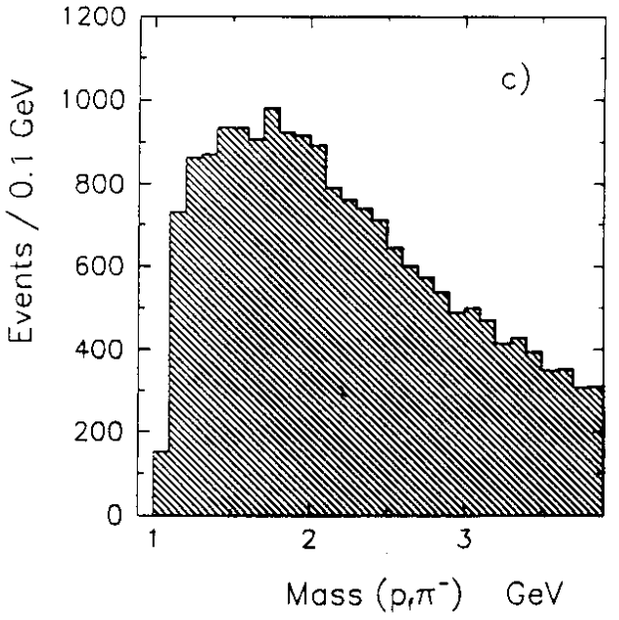
c)
Events / 0.1 GeV
1200
1000
800
600
400
200
0
1
2
3
Mass (p,π⁻) GeV

Fig. 3

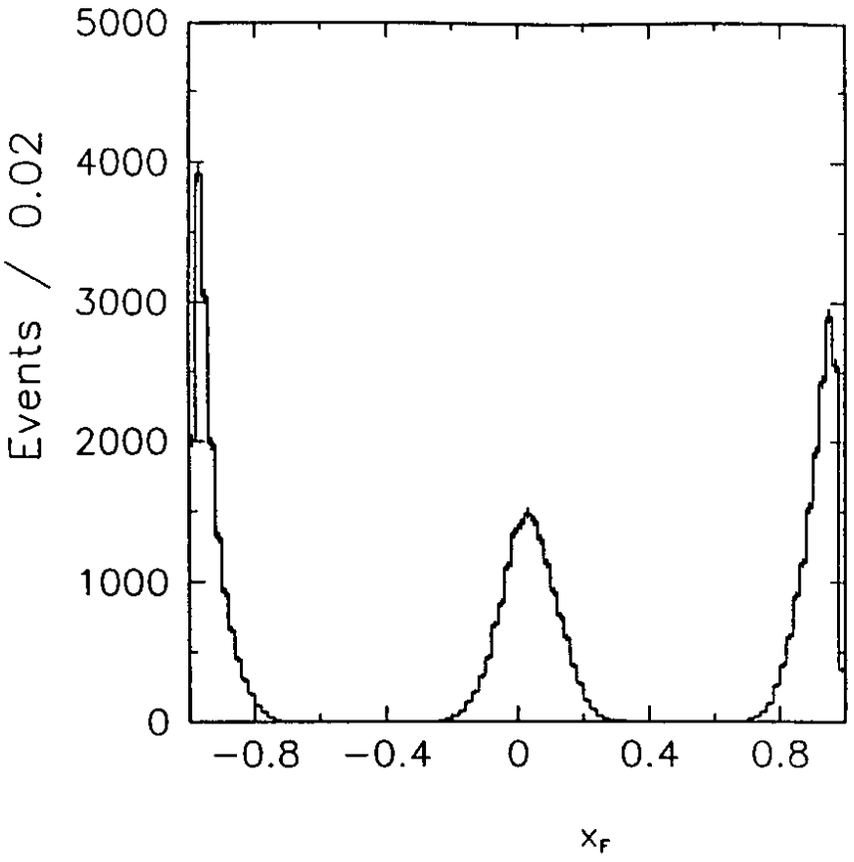

Fig. 4

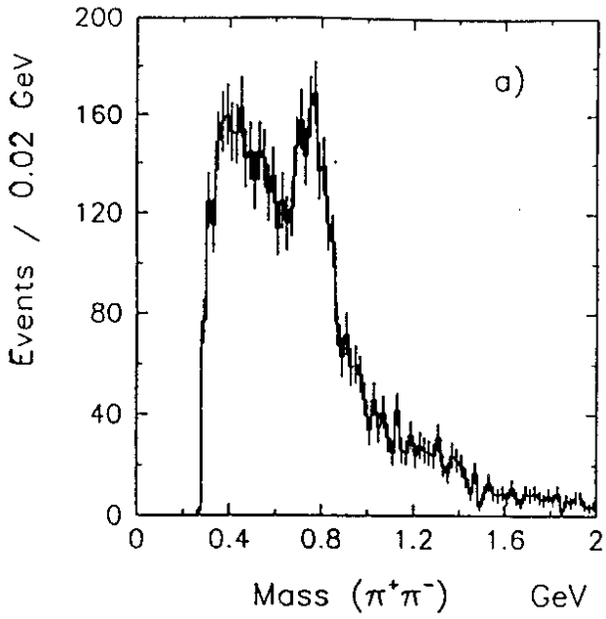
a)
Events / 0.02 GeV
200
160
120
80
40
0
0
0.4
0.8
1.2
1.6
2
Mass $(\pi^+\pi^-)$ GeV

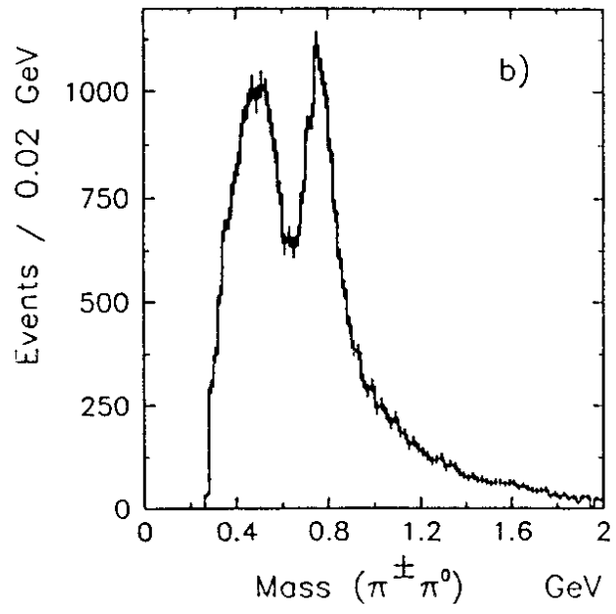
b)
Events / 0.02 GeV
1000
750
500
250
0
0
0.4
0.8
1.2
1.6
2
Mass $(\pi^{\pm}\pi^0)$ GeV

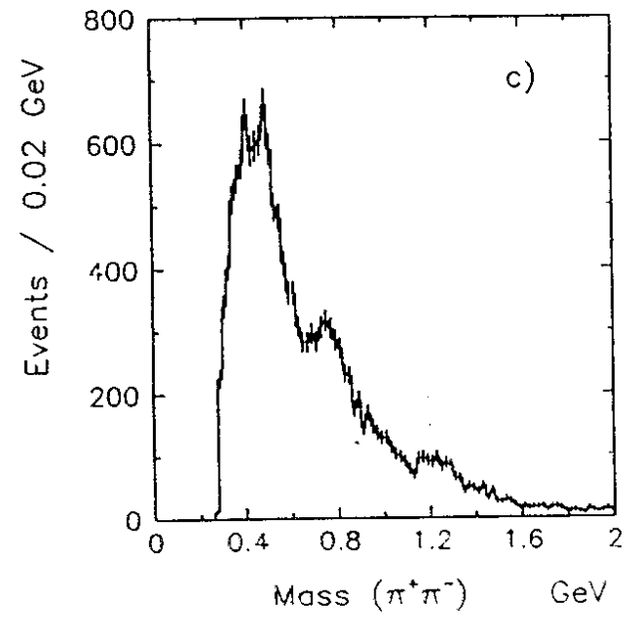
c)
Events / 0.02 GeV
800
600
400
200
0
0
0.4
0.8
1.2
1.6
2
Mass $(\pi^+\pi^-)$ GeV

Fig. 5

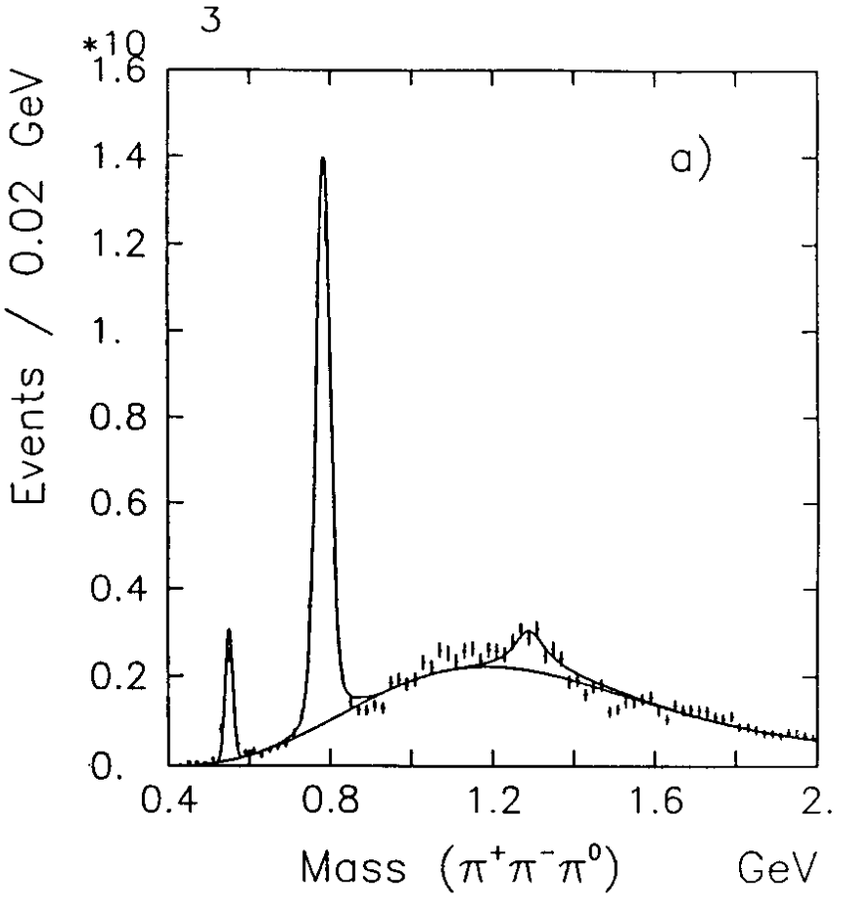
3
*10
1.6
1.4
1.2
1.
0.8
0.6
0.4
0.2
0.
Events / 0.02 GeV
a)
0.4
0.8
1.2
1.6
2.
Mass $(\pi^+\pi^-\pi^0)$ GeV

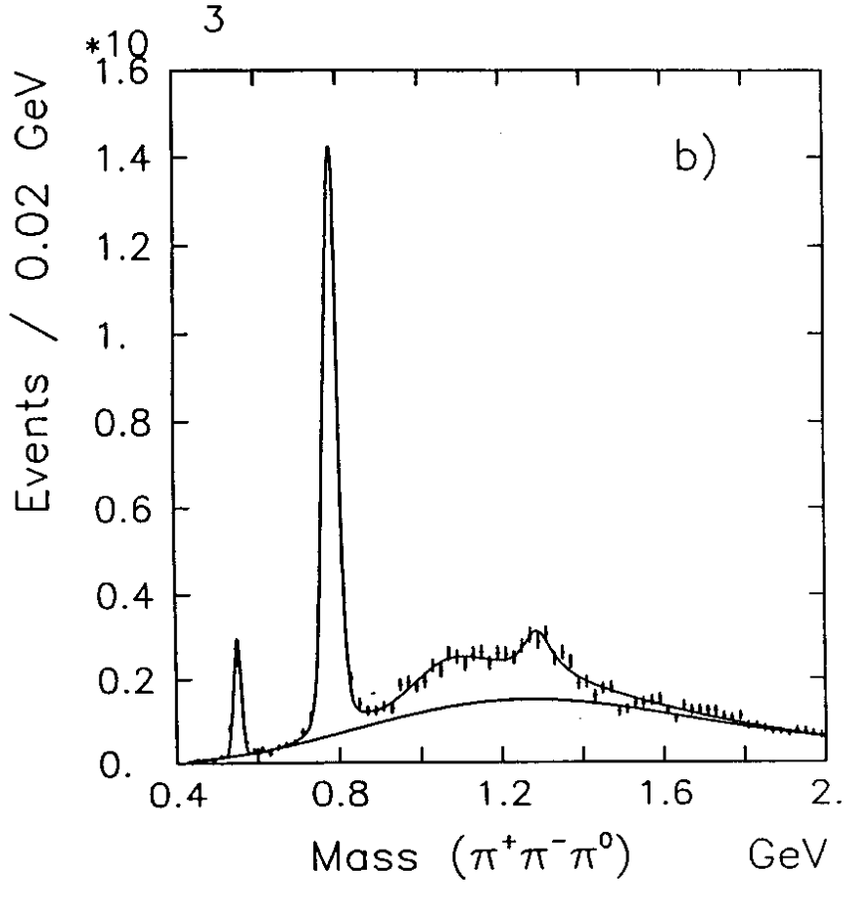
3
*10
1.6
1.4
1.2
1.
0.8
0.6
0.4
0.2
0.
Events / 0.02 GeV
b)
0.4
0.8
1.2
1.6
2.
Mass $(\pi^+\pi^-\pi^0)$ GeV

Fig. 6

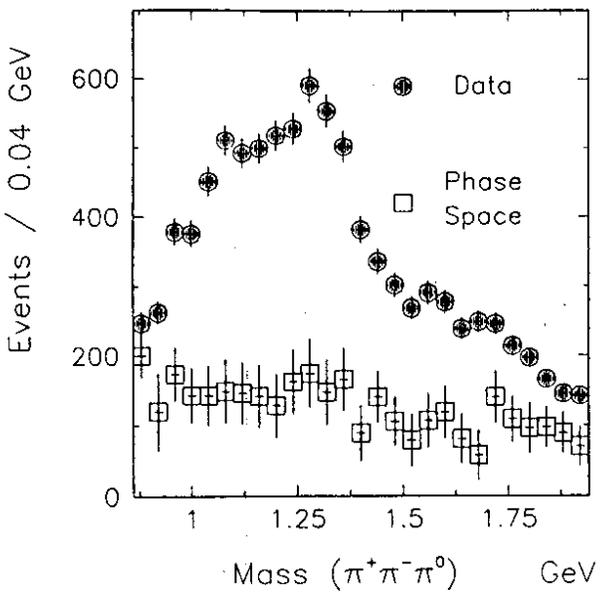
Events / 0.04 GeV
600
400
200
0
Data
Phase
Space
1
1.25
1.5
1.75
Mass $(\pi^+\pi^-\pi^0)$ GeV

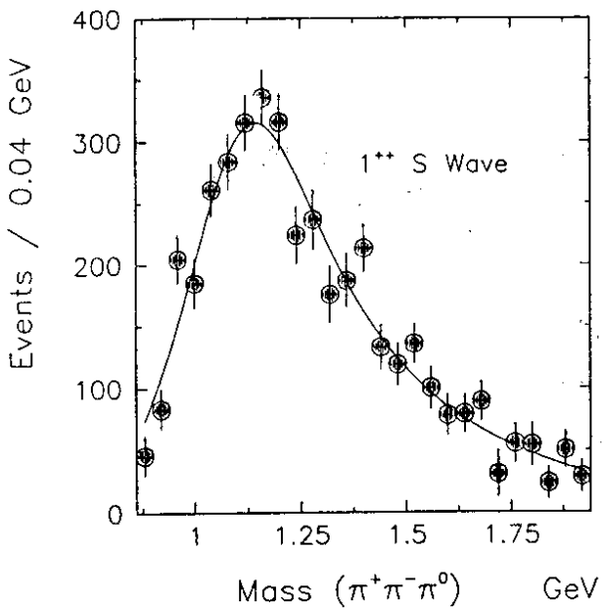
Events / 0.04 GeV
400
300
200
100
0
1^{++} S Wave
1
1.25
1.5
1.75
Mass $(\pi^+\pi^-\pi^0)$ GeV

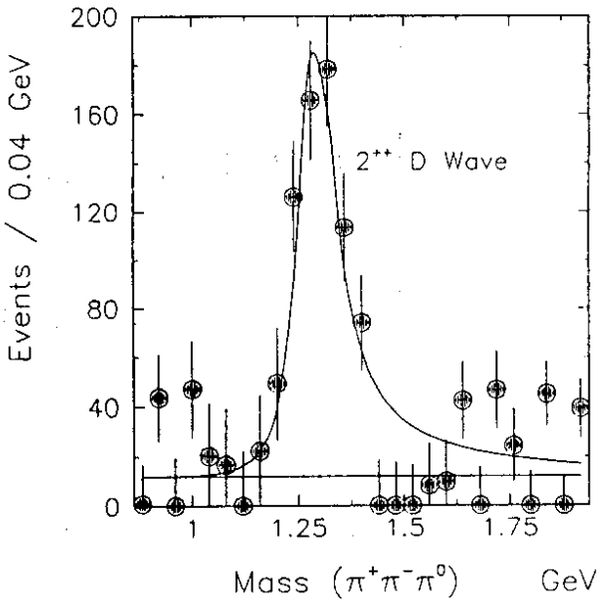
Events / 0.04 GeV
200
160
120
80
40
0
2^{++} D Wave
1
1.25
1.5
1.75
Mass $(\pi^+\pi^-\pi^0)$ GeV

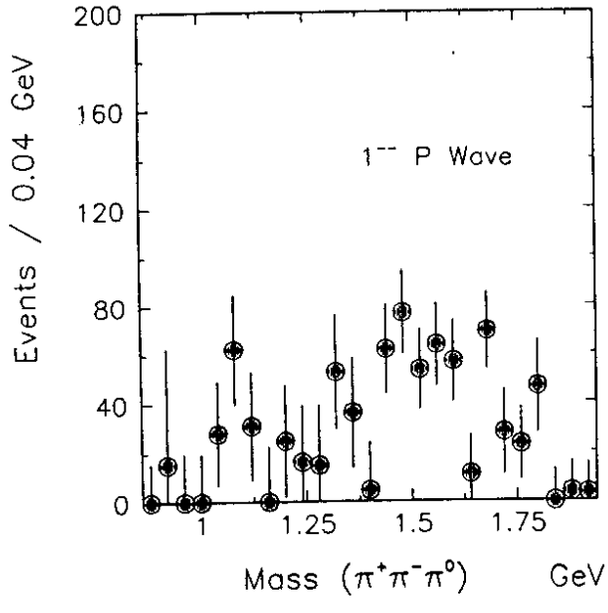
Events / 0.04 GeV
200
160
120
80
40
0
1^{--} P Wave
1
1.25
1.5
1.75
Mass $(\pi^+\pi^-\pi^0)$ GeV

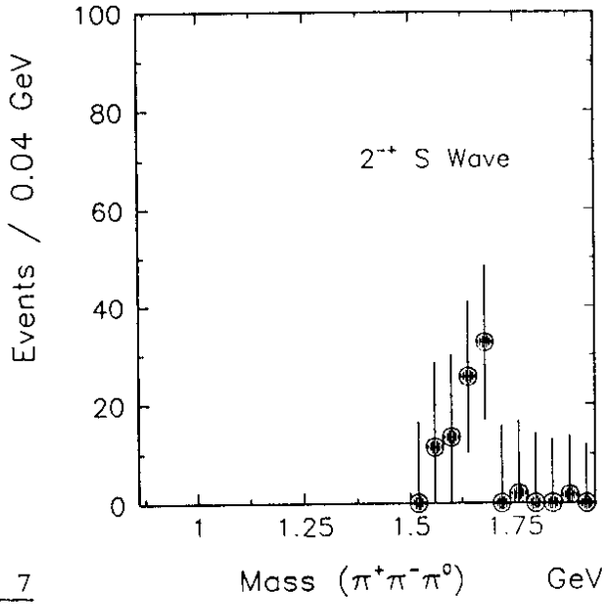
Events / 0.04 GeV
100
80
60
40
20
0
2^{-+} S Wave
1
1.25
1.5
1.75
Mass $(\pi^+\pi^-\pi^0)$ GeV

Fig. 7

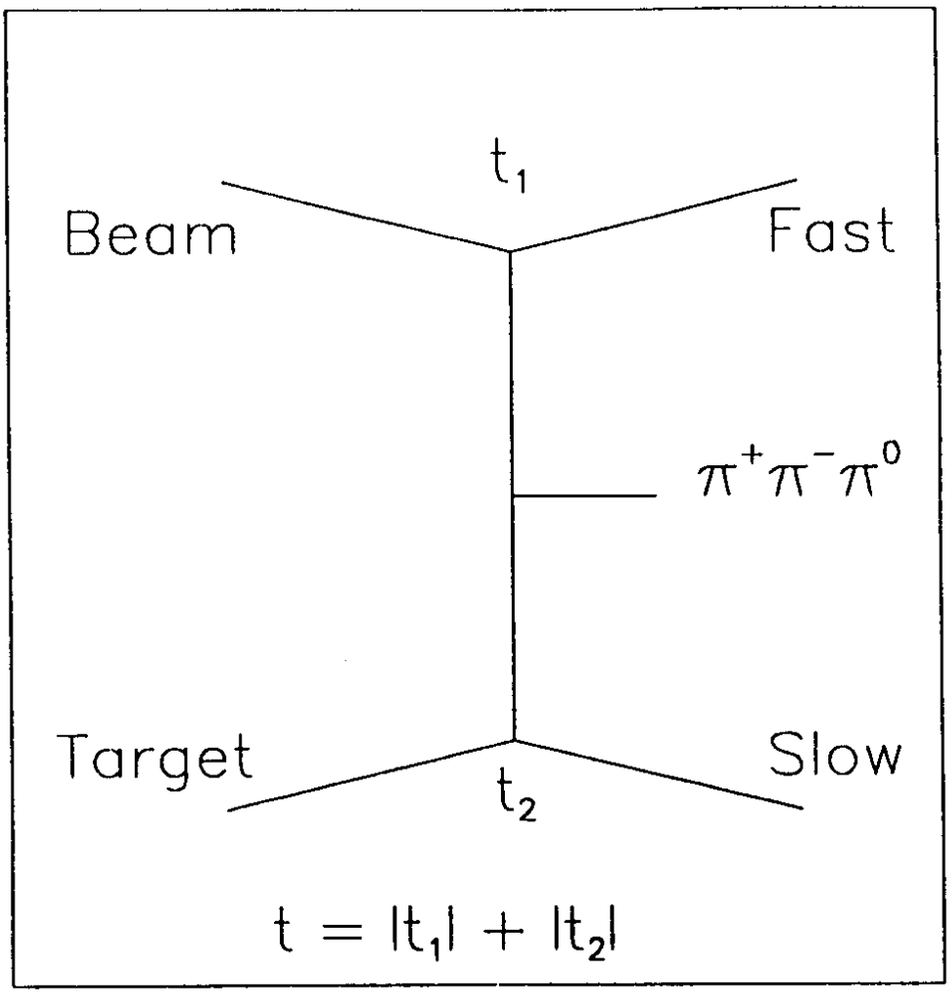

Fig. 8

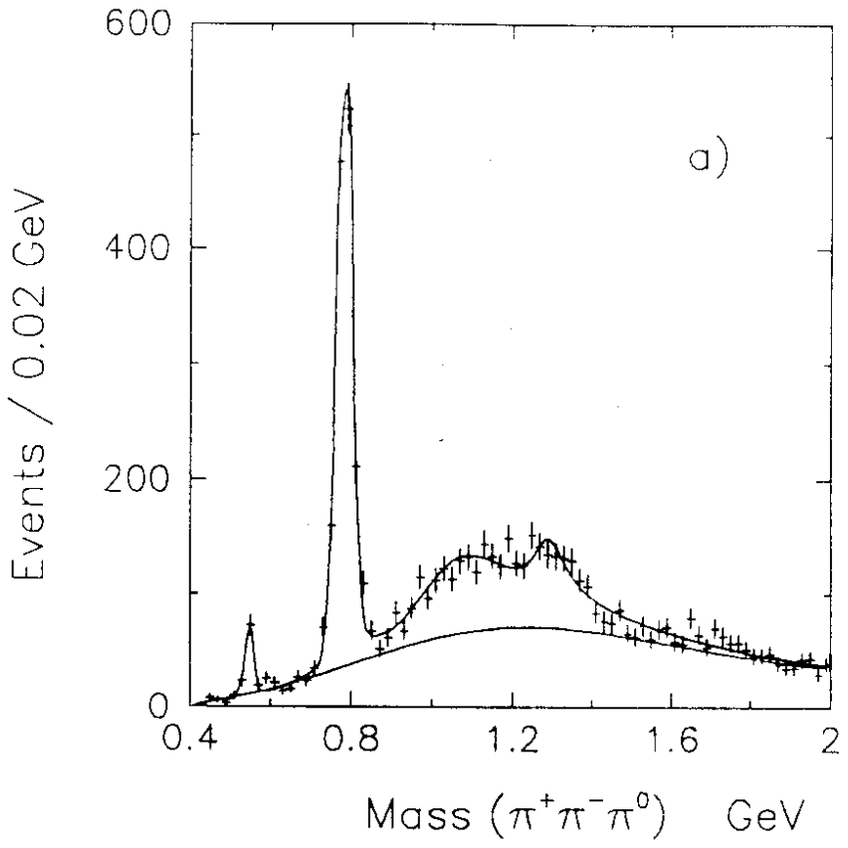
600
400
200
0
Events / 0.02 GeV
a)
0.4
0.8
1.2
1.6
2
Mass ($\pi^+\pi^-\pi^0$) GeV

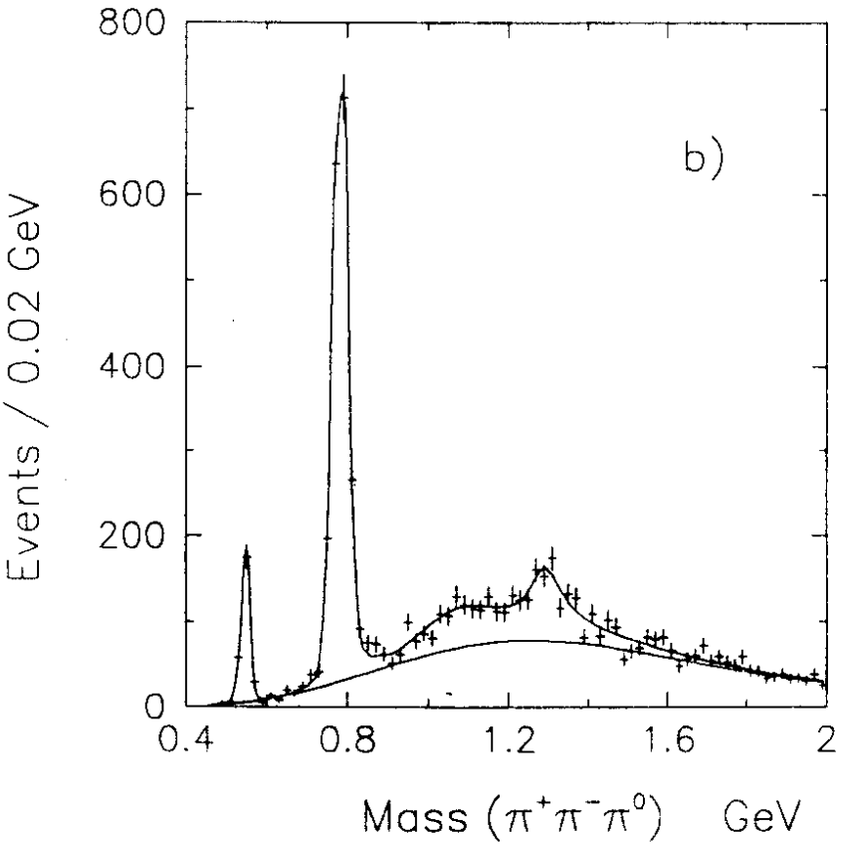
800
600
400
200
0
Events / 0.02 GeV
b)
0.4
0.8
1.2
1.6
2
Mass ($\pi^+\pi^-\pi^0$) GeV

Fig. 9

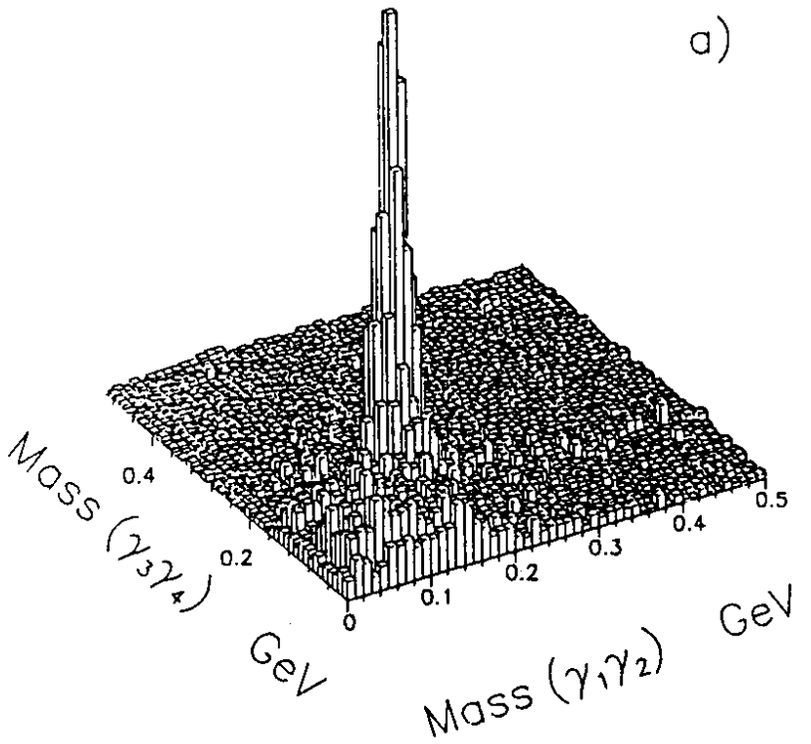
a)
Mass ($\gamma_3\gamma_4$)
GeV
0.4
0.2
0
0.1
0.2
0.3
0.4
0.5
Mass ($\gamma_1\gamma_2$)
GeV

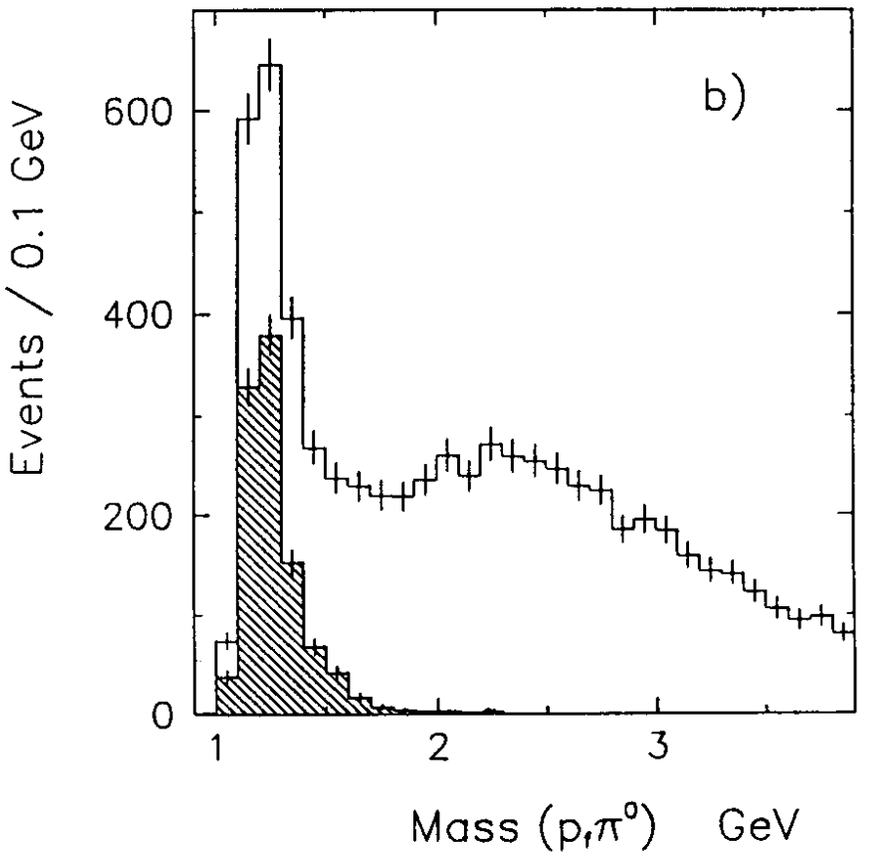
b)
Events / 0.1 GeV
600
400
200
0
1
2
3
Mass ($p_f\pi^0$) GeV

Fig. 10

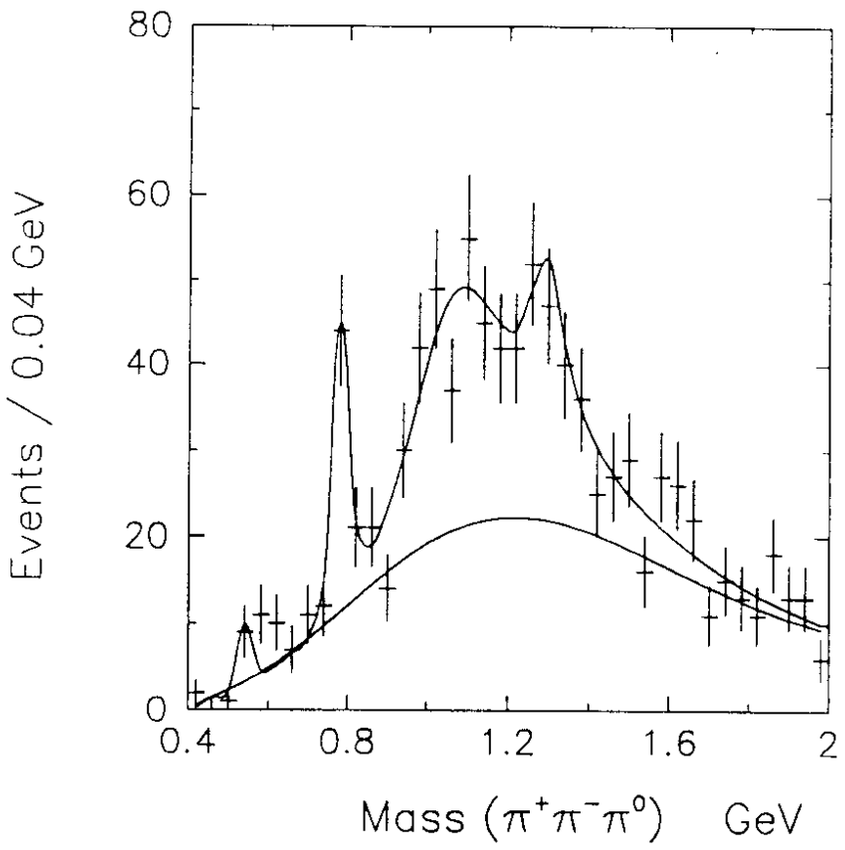

Fig. 11

Imprimé au CERN. Prix : 0.70 Fr.